Journal of Bacteriology

MprAB Regulates the *espA* Operon in Mycobacterium tuberculosis and Modulates ESX-1 Function and Host Cytokine Response

Xiuhua Pang, Buka Samten, Guangxiang Cao, Xisheng Wang, Amy R. Tvinnereim, Xiu-Lan Chen and Susan T. Howard

J. Bacteriol. **2013, 195(1):66. DOI: 10.1128/JB.01067-12. Published Ahead of Print 26 October 2012.**

JB Journals.ASM.org

MprAB Regulates the *espA* Operon in *Mycobacterium tuberculosis* and Modulates ESX-1 Function and Host Cytokine Response

Xiuhua Pang,[a] Buka Samten,[b] Guangxiang Cao,[a] Xisheng Wang,[b] Amy R. Tvinnereim,[c] Xiu-Lan Chen,[a] Susan T. Howard[d]

The State Key Laboratory of Microbial Technology, Shandong University, Jinan, China[a]; Center for Pulmonary and Infectious Disease Control, University of Texas Health Science Center at Tyler, Tyler, Texas, USA[b]; Department of Cellular and Molecular Biology, University of Texas Health Science Center at Tyler, Tyler, Texas, USA[c]; Department of Microbiology, University of Texas Health Science Center at Tyler, Tyler, Texas, USA[d]

The ESX-1 secretion system exports the immunomodulatory protein ESAT-6 and other proteins important in the pathogenesis of *Mycobacterium tuberculosis*. Components and substrates of ESX-1 are encoded at several loci, but the regulation of the encoding genes is only partially understood. In this study, we investigated the role of the MprAB two-component system in the regulation of ESX-1 activity. We determined that MprAB directly regulates the *espA* gene cluster, a locus necessary for ESX-1 function. Transcript mapping determined that the five genes in the cluster form an operon with two transcriptional start points, and several MprA binding sites were detected in the *espA* promoter. Expression analyses and promoter constructs indicated that MprAB represses the *espA* operon. However, the MprAB mutant Rv-D981 secreted lower levels of EspA, ESAT-6, and the ESX-1 substrate EspB than control strains. Secretion of CFP10, which is normally cosecreted with ESAT-6, was similar in Rv-D981 and control strains, further demonstrating aberrant ESX-1 activity in the mutant. ESAT-6 induces proinflammatory cytokines, and macrophages infected with Rv-D981 elicited lower levels of interleukin 1β (IL-1β) and tumor necrosis factor alpha (TNF-α), consistent with the reduced levels of ESAT-6. These findings indicate that MprAB modulates ESX-1 function and reveal a new role for MprAB in host-pathogen interactions.

Mycobacterium tuberculosis has a tremendous global impact on public health, yet the molecular basis of *M. tuberculosis* pathogenesis remains poorly understood. Therefore, the ESX-1 secretion system has stimulated considerable research interest, especially in light of its potential as a drug target (1). ESX-1 is the prototype of type VII secretion systems found in some Gram-positive bacteria (1, 2), and the ESX-1 substrate ESAT-6 is a major virulence factor, implicated in diverse host-pathogen interactions (1, 3), including host cell lysis (4, 5), T cell inhibition (6), and activation of macrophage inflammasomes (7, 8). The protein CFP10 is cosecreted with ESAT-6, forming a 1:1 complex, and interacts with the secretion apparatus (9–11). ESAT-6 and CFP10 are encoded within the *M. tuberculosis* RD1 region that contains genes for structural components of the ESX-1 secretion apparatus and other ESX-1 substrates (3, 4, 11–13). Loss of ESAT-6 attenuates *M. tuberculosis*, and deletion of multiple other genes in the RD1 region impairs ESX-1 function and virulence (3, 4, 9, 14, 15).

Another locus critical for ESX-1 function contains the *espA* operon, with genes encoding the secreted proteins EspA (Rv3616c), EspC (Rv3615c), and EspD (Rv3614c) (16–18). Secretion of EspA and ESAT-6 is mutually dependent, with deletion of *espA* resulting in loss of ESAT-6 secretion and attenuation (17). Disruption of disulfide bond formation in EspA retains ESX-1 function but produces a severely attenuated strain, indicating that EspA is itself a major virulence determinant (19). EspC contains a signal sequence required for secretion of EspA and ESAT-6 (20), and EspD stabilizes cellular levels of EspA and EspC (16). Two downstream genes, Rv3613c and Rv3612c, are not required for ESX-1 function (21) but sometimes share *espA* expression patterns (22, 23).

Transcriptional regulators of ESX-1 include EspR, which activates the *espA* operon (21) and which was recently reported to be a nucleoid-associated protein involved in global gene regulation (24). EspR binds the *espA* promoter (25, 26), and an EspR mutant exhibited decreased transcription of the *espA* operon, loss of ESAT-6 secretion, and reduced virulence (21). The two-component system (TCS) PhoPR also activates the *espA* operon (27). Evidence suggests that PhoPR senses low pH (28), consistent with the upregulation of the *espA* operon by acidic conditions (29). CRP represses the *espA* operon (23), and the nucleoid-associated protein Lsr2 binds within the RD1 region and *espA* operon, repressing transcription (30).

Here, we report that the *espA* operon is directly regulated by the MprAB TCS. MprAB activates the response to envelope stress induced by surfactants (22, 31). The response regulator MprA binds a repeated hexamer motif (MprA box) found primarily in the promoters of genes associated with envelope stress (22, 31–35). The majority of these promoters are activated by MprAB, but MprAB can also repress expression under some conditions (34). Previous DNA microarray studies revealed that *espA* and the downstream genes Rv3615c to Rv3612c were derepressed in our *mprAB* mutant, Rv-D981 (22). We further explored this finding and discovered that MprAB is required for ESX-1 function.

Received 14 June 2012 Accepted 18 October 2012

Published ahead of print 26 October 2012

Address correspondence to Susan T. Howard, susan.howard@uthct.edu, or Xiuhua Pang, pangxiuhua@sdu.edu.cn.

B.S. and G.C. contributed equally to this work.

Supplemental material for this article may be found at http://dx.doi.org/10.1128/JB.01067-12.

doi:10.1128/JB.01067-12

MATERIALS AND METHODS

Bacterial strains and culture conditions. Rv-D981 is an *mprAB* deletion mutant of *M. tuberculosis* strain H37Rv, and Rv-D981COM is the *mprAB*-complemented strain (22). ST100 is a *phoP* mutant of H37Rv (27). Due to differences in H37Rv strains, we have designated the parental strain of ST100 as H37Rv-2. Strains were grown in Middlebrook 7H9 broth containing 0.05% Tween 80 and 10% oleic acid-albumin-dextrose-catalase (OADC) at 37°C with shaking under atmospheric CO_2. *Escherichia coli* NovaBlue and Rosetta(DE3)pLysS (Novagen) were used for general cloning and protein expression, respectively.

RNA isolation, reverse transcription, and real-time PCR. Procedures were conducted essentially as described previously (22). Briefly, *M. tuberculosis* strains were grown to mid-exponential phase and total RNA was extracted by bead beating, followed by further purification and DNase treatment. Following reverse transcription (RT) with random hexamer primers and Moloney murine leukemia virus (MMLV) reverse transcriptase, real-time PCR assays were performed with gene-specific primers and probes, using an ABI Prism 7300 thermal cycler. Relative quantities of cDNA were determined from standard curves generated using genomic DNA and were normalized for 16S rRNA. Sequences of primers and probes used in this study are listed in Table S1 in the supplemental material.

Primer extension analysis. Primer extension was performed with primers Rv3616c Ext-1, Rv3616cR3 and Rv3616c Ext-3 essentially as described previously (33), using a high-temperature-tolerant reverse transcriptase and high annealing and extension temperatures to overcome possible secondary structures. Reaction products were separated on 8% polyacrylamide sequencing gels, alongside sequencing reactions performed with the same primer.

RLM-RACE. The FirstChoice RNA ligase-mediated rapid amplification of cDNA ends (RLM-RACE) kit (Ambion) was used with the manufacturer's recommended protocol. Briefly, H37Rv total RNA was extracted at mid-exponential phase. Following dephosphorylation, RNA was ligated to a 45-base RNA adaptor, followed by random-primed reverse transcription. Reactions were also run in parallel without reverse transcriptase to control for the presence of genomic DNA. The 5′-RACE outer primer (Ambion) and primer Rv3616c-R9 were used for outer PCR. Next, for inner PCR, the 5′-RACE inner primer was paired with either Rv3616c-Ext1 (TSP1) or Rv3616c-R3 (TSP2). PCR products were analyzed on an agarose gel, and specific bands were excised and sequenced.

Protein extraction and Western blotting. *M. tuberculosis* strains were grown in 7H9 to an optical density at 600 nm (OD_{600}) of 0.3 to 0.4, centrifuged, washed, and then suspended in Sauton's medium at an OD_{600} of 0.1. At different time points, cell pellets and supernatants were collected by centrifugation to prepare cell lysates and culture filtrates (secreted proteins), respectively. Cell pellets were washed and then disrupted by bead beating. Cell debris was removed by centrifugation, and lysate supernatants were collected for analysis.

To obtain secreted proteins, supernatants from the initial centrifugation were filtered through 0.20-μm filters (Millipore) and concentrated using a centrifugal filter unit with a 3-kDa cutoff (Millipore), followed by buffer exchange into 50 mM Tris-HCI, 50 mM NaCI buffer, pH 8.0.

Protein concentration was determined by bicinchoninic acid (BCA) assay (Pierce). Proteins were separated using a 15% polyacrylamide gel under denaturing and reducing conditions. For immunoblotting, we used the Western ECL detection system (Amersham) with antibodies to ESAT-6 (monoclonal antibody [MAb] HYB 076-08, a gift from Peter Andersen), EspA (a gift from Sarah Fortune), EspB (AB43671; Abcam), CFP-10 (NR13801; BEI Resources), Mpt32 (NR13817; BEI Resources), and GroEL2 (NR-13655; BEI Resources).

Construction of promoter fusion plasmids and assays. *espA* promoter regions were inserted upstream of the β-galactosidase gene *lacZ* in plasmid pSM128 (36) (a gift from Issar Smith). The full-length intergenic region was amplified using primers Rv3616c-FuF1/Rv3616c-FuR1 (construct P1). Partial intergenic regions of 976 bp, 585 bp, and 429 bp were amplified, respectively, using forward primers Rv3616c-Fu-976 (construct P2), Rv3616c-Fu-585 (construct P3), and Rv3616c-Fu-429 (construct P4), with reverse primer Rv3616c-FuR1. Primers included an *Sca*I site for cloning into pSM128. Insert orientation was verified by sequencing.

For β-galactosidase analysis, promoter fusion plasmids and the control vector pSM128 were electroporated into H37Rv and Rv-D981. Transformants were selected in the presence of streptomycin (50 μg/ml) and confirmed by PCR analysis. Cell lysates were prepared by bead beating essentially as described previously (37) and then filtered. Protein concentration was determined by the BCA assay, and β-galactosidase activity was measured in Miller units (nanomoles of nitrophenol produced per minute per milligram of protein), as described previously (37, 38). For statistical analyses, an unpaired two-tailed *t* test was performed using GraphPad software.

EMSAs. MprA was expressed in *E. coli*, and electrophoresis mobility shift assays (EMSAs) were conducted, as described previously (22, 33). Briefly, DNA probes were amplified by PCR, or for short probes containing putative MprA boxes, complementary 45-mer oligonucleotides were annealed. Probes were end labeled with [γ-^{32}P]ATP and incubated with MprA, with or without specific or nonspecific cold (unlabeled) probes. Reaction mixtures were analyzed on nondenaturing polyacrylamide gels, and bands were detected by autoradiography.

Macrophage infection and cytokine analysis. Blood samples were collected from seven healthy employees at UTHSCT, upon obtaining signed consent forms and according to protocols approved by the Institutional Review Board. Preparations of human mononuclear phagocytes and *M. tuberculosis* infections were performed essentially as described previously (39). Peripheral blood mononuclear cells were isolated using Ficoll-Paque PLUS (Amersham Biosciences) and resuspended in RPMI 1640 supplemented with 10% pooled human AB serum (Atlanta Biologicals) in 24-well plates. After 1 h, nonadherent cells were removed by washing. Adherent cells were cultured in macrophage serum-free medium (Gibco) for 5 days to differentiate into macrophages. This method results in 1×10^6 macrophages/well with over 95% purity. Cells were infected with single-cell suspensions of *M. tuberculosis* strains at a multiplicity of infection (MOI) of 5 or 10. At different time points, culture supernatants were harvested, filtered through a 0.2-μm syringe filter, and stored at −70°C. Cytokine concentrations were measured by enzyme-linked immunosorbent assay (ELISA) using capture and detection antibodies for tumor necrosis factor alpha (TNF-α) (BD Biosciences) and ELISA kits for interleukin 8 (IL-8) and IL-10 (R&D Systems) and IL-1β (Mabtech), with a lower detection limit of 15 to 25 pg/ml. Paired Student's *t* test or Wilcoxon matched-pairs signed-rank tests were used for statistical analysis.

RESULTS

Expression of ESX-1-associated genes in an *mprAB* mutant. Our previous DNA microarray analyses indicated that *espA* and *espD* expression was derepressed in the *mprAB* mutant Rv-D981 compared to expression in the parental strain H37Rv (22). For a more precise comparison, we performed real-time PCR and determined that each gene was expressed at 5-fold-higher levels in Rv-D981 than in H37Rv (Fig. 1). Restoration of *mprAB* in the complemented strain Rv-D981COM resulted in expression levels similar to those found in H37Rv, confirming that MprAB represses expression of *espA* and *espD*. Expression of *esxA*, which encodes ESAT-6, was similar between the three strains (Fig. 1), indicating that MprAB does not regulate this gene under normal growth conditions.

Transcriptional analyses of the *espA* operon. To delineate transcription in the *espA* region, we identified transcriptional start points (TSPs). Primer extension analysis localized TSP1 within a row of cytosines approximately 65 bp upstream of the predicted

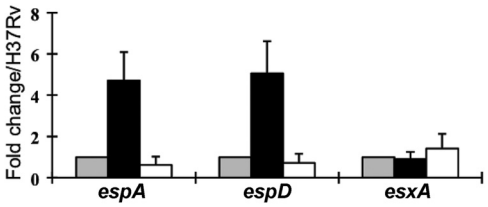

FIG 1 Regulatory effect of *mprAB* on three genes of the ESX-1 secretion system. Expression of *espA* (Rv3616c), *espD* (Rv3614c), and *esxA* (ESAT-6) was examined by real-time PCR using RNA extracted from H37Rv (gray bars), Rv-D981 (black bars), and Rv-D981COM (white bars) during exponential-phase growth. Results were normalized for 16S RNA and are shown as fold change over the results for the H37Rv control, which was given the value of 1 for each gene. Data are the means ± standard deviations (SD) from three separate experiments.

start codon (Fig. 2A). 5′-RACE analysis with primer Rv3616c Ext-1 (Fig. 2B, lane 4) localized TSP1 as the first cytosine, at position −67 (Fig. 2D), consistent with a recent study (40). Use of the upstream primer Rv3616c-R3 in 5′-RACE generated another amplicon (Fig. 2B, lane 5), sequence analysis of which identified a second TSP at position −169 (Fig. 2D). TSP2 has not been previously reported. Therefore, we confirmed its location by primer extension analysis with primer Rv3616c-Ext3 (Fig. 2C and D) and two additional primers (data not shown). The sequence GACGA upstream of TSP2 (Fig. 2D) is also present just upstream of the *mprA* TSP (22) and is a potential −10 box.

espA and *espD* belong to a cluster of five genes with similar expression patterns in Rv-D981 (22), so we used RT-PCR to determine whether the genes are cotranscribed (Fig. 2E and F). Transcripts were detected between *espA* and *espC* using primers P1 and P2, and analyses with other primer pairs revealed transcription across each of the downstream intergenic regions (Fig. 2F). These results confirmed a recent report that Rv3616c to Rv3612c comprise a single operon (40). However, the band generated by primers P7 and P8 was very weak, suggesting that some transcripts are not extended fully through the operon or that the 3′ ends of the transcripts have reduced stability, possibly as a regulatory mechanism.

MprA binds the *espA* promoter. To determine whether MprA directly regulates the *espA* operon, probes were generated to proximal and distal regions of the *espA* promoter (Fig. 3A) to test for MprA binding. Both probes were shifted by MprA in EMSAs (Fig. 3B and C), and a gradual retardation of these probes was observed with increasing MprA concentrations, particularly with the proximal promoter probe (Fig. 3B). We have previously observed this stepwise shift with promoters that contain multiple MprA binding sites (MprA boxes) (33, 34).

Screening of the *ephA-espA* intergenic region for sequences similar to the MprA box consensus (22, 32) revealed several potential boxes (Fig. 3A and D; see also Fig. S1 in the supplemental material), five of which mapped within either the distal or proximal probes (Fig. 3A). EMSAs were conducted with 45-mer probes containing the individual boxes (Fig. 3D to G). Boxes 1, 2, 3, and 7 did not show detectable MprA binding (Fig. 3D, G, and data not shown), although they may be auxiliary sites that enhance MprA binding to other MprA boxes, similar to sites found in other MprA-regulated promoters (31, 33). However, boxes 4 and 5 bound MprA (Fig. 3D to F), and box 6 was also shifted by MprA, albeit very weakly (Fig. 3G). Overall, binding of MprA to individual boxes was markedly weaker than to the distal and proximal probes, which contained more than one predicted MprA box (Fig. 3A to C). Cooperativity between boxes may contribute to the stronger binding observed with the larger probes. Additionally, the proximal and distal probes potentially contain other MprA boxes not detected by our screening. Considerable variation from the consensus sequence for MprA boxes can occur, particularly with weak or auxiliary MprA binding sites (31–34).

We verified the location of boxes 4 and 5 by generating mutations within the half-sites or spacer region (Fig. 3E and F, probes m1 to m3). No binding was detected with mutations m2 and m3 for box 4 (Fig. 3E) or with any of the mutations for box 5 (Fig. 3F), suggesting that the predicted boxes are correct. On long exposures, a weak band was detectable with mutation m1 for box 4 (data not shown), which included a deletion in the spacer region. This shift was surprising given that deletions in the spacer region usually disrupt MprA binding (32). However, it is possible that the deletion generated a cryptic MprA binding site not present with the other mutations.

Analysis of *espA* promoter regions. To define critical portions of the *espA* promoter and to further evaluate the role of MprA in regulation, *lacZ*-promoter fusion constructs were generated (Fig. 4A) and used to transform H37Rv and Rv-D981. β-Galactosidase activity was conducted on cell lysates and compared to the vector controls (Fig. 4B). In H37Rv, the highest β-galactosidase activity was observed with construct P1, which contains the entire intergenic region. We anticipated that *lacZ* expression levels from P1 would be higher in Rv-D981 than H37Rv, given that *espA* was derepressed in Rv-D981 by quantitative PCR (qPCR) (Fig. 1) and DNA microarray analyses (22). In contrast, β-galactosidase activity was lower in the mutant (Fig. 4B). The basis for this unexpected finding is unclear. However, we speculate that the region upstream of the intergenic region contains regulatory sites that enhance *espA* transcription in the absence of MprAB but which are missing from the P1 construct. MprAB may also downregulate a secondary repressor that binds in the P1 promoter region, leading to the lower expression levels observed in Rv-D981. Additional studies are required to clarify this issue.

Activity with the P2 construct was more consistent with anticipated results. In H37Rv, *lacZ* expression from P2 was significantly reduced compared to that from P1 (Fig. 4B), likely due to loss of EspR site C (see Fig. S1 in the supplemental material), a major EspR-activating site (26). P2 is also missing most of the *espA*-activating region that lies between bases −884 to −1004 and that overlaps EspR site C (40). In contrast to H37Rv, P2 generated the highest β-galactosidase activity in Rv-D981, with levels nearly 3-fold higher than in H37Rv (Fig. 4B). MprA boxes 1 and 2 were deleted from P2, but the construct retained five MprA boxes potentially involved in repression, including boxes 4 to 6 that exhibited MprA binding (Fig. 3D to G). The elevated activity of P2 in Rv-D981, despite the loss of EspR site C, suggests that a major role of EspR is to overcome transcriptional repression by MprA.

Construct P3, which is missing both EspR sites B and C, generated β-galactosidase activity in H37Rv similar to that for P2, which is missing only EspR site C (Fig. 4B; see also Fig. S1 in the supplemental material). The EspR sites function cooperatively (26), and this may explain why no further reduction in activity was observed, although other studies have reported diminished activity with loss of EspR sites A or B (21, 40). The difference between H37Rv and Rv-D981 was smaller with P3 than with P2 (Fig. 4B),

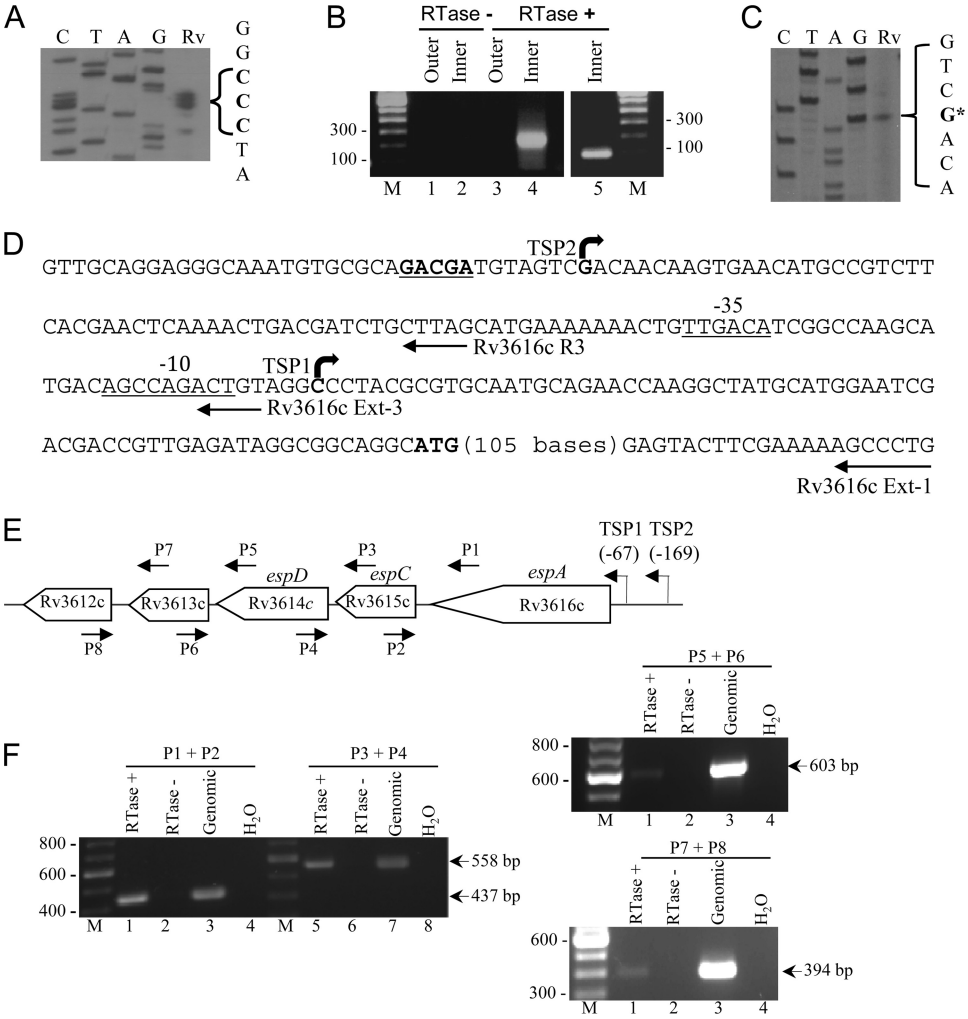

FIG 2 Transcriptional mapping of the *espA* operon. RNA was extracted from H37Rv during exponential-phase growth. (A) TSP1 was mapped by primer extension using primer Rv3616c Ext-1. The same primer was used to generate the sequence ladder. Bolded letters correspond to the short ladder of bands detected for H37Rv (Rv). (B) Identification of TSP1 and TSP2 by 5′-RACE. RNA was incubated without (lanes 1 and 2) or with (lanes 3, 4, and 5) reverse transcriptase (RTase), and the resulting cDNA was ligated to an adaptor. The cDNA ends were first amplified using an outer set of primers to the adaptor and *espA*, followed by reamplification with inner (nested) primers. TSP1 and TSP2 were identified from amplicons generated with an inner primer to the adaptor paired, respectively, with (lane 4) primer Rv3616c Ext-1 and (lane 5) primer Rv3616cR3. The inner adaptor primer and Rv3616c Ext-1 were also used in PCR to confirm the absence of chromosomal DNA (lane 2). M, 100-bp ladder. (C) Primer extension analysis of TSP2. Analysis was performed using primer Rv3616c Ext-3, as described for panel A. The asterisk marks the nucleotide corresponding to TSP2. (D) Locations of TSPs in the *espA* promoter. TSP1 and TSP2 are marked by curved arrowheads and a bolded nucleotide and are located at positions −67 and −169 with respect to the *espA* start codon (bolded ATG). The −35 and −10 boxes for TSP1 (40) are underlined. Bolded, underlined bases denote the potential −10 box for TSP2 that matches the sequence upstream of the *mprA* TSP (22). The locations of primers used in TSP mapping are indicated by arrows below the corresponding line of sequence. (E) Schematic representation of the DNA region comprising *espA* (Rv3616c) through Rv3612c. Location and orientation of primers P1 to P8 used in RT-PCR analysis in panel F are marked. TSPs identified in this study are identified by bent arrows. (F) Rv3616c to Rv3612c are cotranscribed. Reverse transcription was conducted with (lanes 1 and 5) or without (lanes 2 and 6) reverse transcriptase, and then PCR was performed with primers P1 to P8 to detect transcripts between adjacent genes. Genomic DNA (lanes 3 and 7) and distilled water (lanes 4 and 8) were included, respectively, as positive and negative PCR controls. To enhance the visibility of the band generated by primers P7 and P8, the entire panel was lightened using image contrast.

possibly due to loss of the potential repressor sites MprA box 4 and box 3 from P3 (see Fig. S1 in the supplemental material). However, confirmation of the role of these sites and the other MprA boxes in *espA* repression requires further analyses.

Promoter activity from construct P4 trended higher than that from P3, with a significant difference observed in H37Rv (H37Rv, $P < 0.05$; Rv-D981, $P = 0.047$) (Fig. 4B). P4 contains a 429-bp section of the *espA* promoter and was the shortest region we tested (Fig. 4A). Using *espA* promoter-*lacZ* constructs in *Mycobacterium smegmatis*, Hunt et al. (40) demonstrated a small increase in activity with a similar 427-bp region, compared to regions of 464-bp and 217-bp. Their 427-bp promoter construct also showed higher activity than the 217-bp promoter construct in *M. tuberculosis* (40). These findings suggest that the region between −429 and −217 contains an activation site that is normally repressed in the presence of upstream sequences. Interestingly, P4 retains two MprA boxes, boxes 5 and 6, yet there was only a small elevation in activity in Rv-D981 compared to that in H37Rv. It is possible these are only weak repression sites and/or that *espA* repression involves cooperation with upstream MprA boxes.

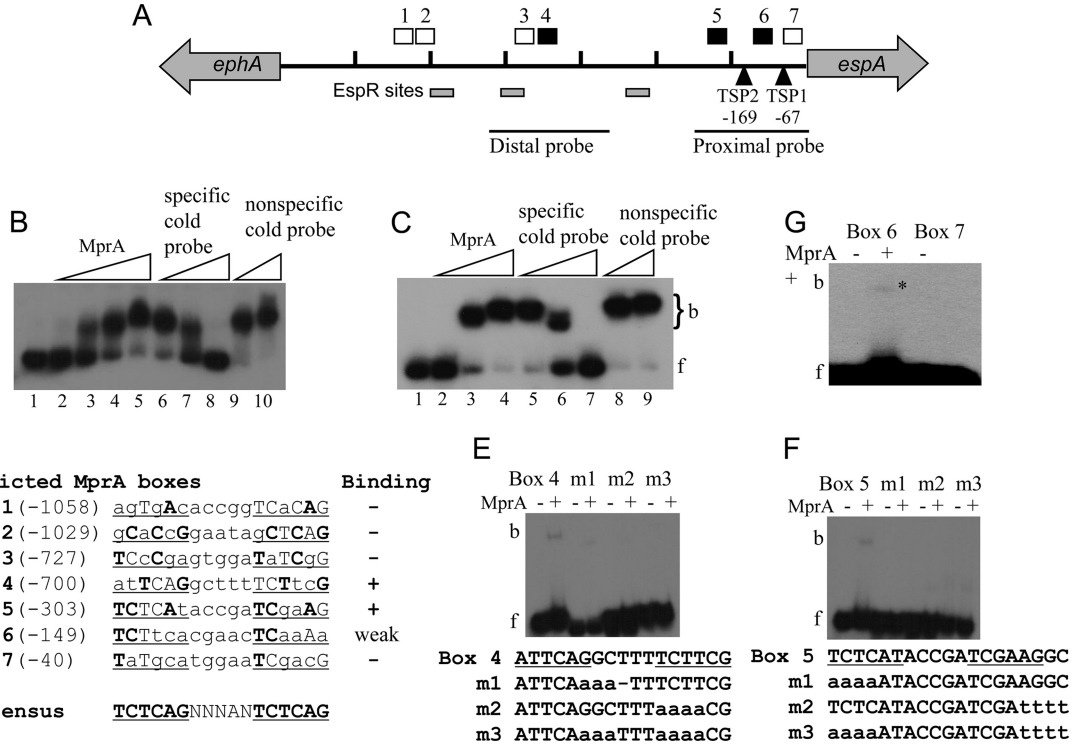

FIG 3 MprA binds the *ephA-espA* intergenic region. (A) Schematic diagram of the *ephA-espA* intergenic region. Vertical bars mark 200-bp increments from the *espA* start codon. Predicted MprA boxes are numbered, and those confirmed by EMSAs are in black. Flat gray boxes represent EspR sites. The locations of the proximal and distal probes used, respectively, in panels B and C are indicated. Short vertical arrowheads denote TSPs, and positions are shown relative to the *espA* start codon. (B) Proximal promoter. The 342-bp proximal promoter probe extends from −312 to the *espA* start codon and was generated with primers Rv3616c-F2/R1. The radiolabeled probe was incubated with no MprA (lane 1); 0.45 to 3.6 μg MprA (lanes 2 to 5); 3.6 μg MprA and 70-fold, 210-fold, or 420-fold excess of unlabeled specific probe (lanes 6 to 8); 3.6 μg MprA and 210-fold or 420-fold excess of unlabeled nonspecific probe (lanes 9 and 10). (C) Distal promoter. The 380-bp distal promoter probe extends from −848 to −468 and was generated with primers Rv3616c-F7/R2. The radiolabeled probe was incubated with no MprA (lane 1); 0.55 to 3.3 μg MprA (lanes 2 to 4); 3.3 μg MprA and 120-fold, 240-fold, or 480-fold excess of unlabeled specific probe (lanes 5 to 7); 3.3 μg MprA and 180-fold or 360-fold excess of unlabeled nonspecific probe (lanes 8 and 9). (D) Predicted MprA boxes were identified based on similarity to the published consensus sequence. Bases matching the consensus sequence are capitalized, and those present in each half-site are bolded. Half-sites are underlined. Numbers indicate the position of the first base relative to the *espA* start codon. Forty-five-base-pair probes containing the boxes showed strong (+), weak, or no (−) binding to MprA in EMSAs, as indicated. (E and F) EMSAs with predicted MprA boxes 4 to 7. Short radiolabeled probes containing each box were incubated with (+) or without (−) 6 μg MprA. For box 4 (E) and box 5 (F), probes with the indicated mutations (m1, m2, m3) were tested for MprA binding. Small letters and the dash mark indicate altered nucleotides and a deletion, respectively. (G) Boxes 6 and 7. An asterisk marks the shifted band containing box 6. f, free probe; b, bound probe, for all panels.

Effects of MprAB on the ESX-1 secretion system. Our transcriptional analyses indicated that MprA represses the *espA* operon. Therefore, we anticipated that Rv-D981 would overexpress EspA. Synthesis and secretion of EspA were examined using Rv-D981 and control strains and an anti-EspA antibody (Fig. 5). Surprisingly, Western blot analysis of culture filtrates (secreted proteins) demonstrated that Rv-D981 exported lower levels of EspA than control strains, with EspA only weakly detectable by day 7 (Fig. 5A). The defect in EspA secretion in Rv-D981 was not reflected in cell lysates, which showed levels of EspA similar to those of control strains (Fig. 5B). These results contrasted with lysates of the *phoP* mutant ST100 in which EspA was barely detectable (Fig. 5B), indicating that MprAB and PhoPR have differing regulatory effects on ESX-1 proteins.

Since EspA is required for ESX-1 function (16–18), we investigated whether Rv-D981 also secreted smaller amounts of other ESX-1 substrates (Fig. 5A). Secretion of ESAT-6 was greatly reduced in Rv-D981 compared to that in control strains (Fig. 5A), consistent with the mutually dependent secretion of ESAT-6 and EspA (17). ESAT-6 levels were similar in lysates of Rv-D981 and control strains (Fig. 5A), so, as with EspA, ESAT-6 is synthesized in Rv-D981, but secretion is aberrant. Rv-D981 also secreted lower levels of EspB (Rv3881c), indicating a broad effect of MprAB on ESX-1 function. The observed differences in secreted proteins were not due to differential cell lysis among the strains, as the cytosolic protein GroEL2 was not detected in any of the culture filtrates (Fig. 5A, bottom). Additionally, Rv-D981 does not appear to have a general defect in protein export, as evidenced by the normal extracellular levels of Mpt32, a protein secreted independently of ESX-1 (41).

It is notable that in contrast to other ESX-1 proteins, secretion of the substrate CFP10 was not reduced in Rv-D981 (Fig. 5A). This result revealed a surprising disassociation between ESAT-6 and CFP10 activity in the *mprAB* mutant, as these proteins are usually cosecreted in a one-to-one ratio (10). Overall, our analyses indicate that there is a major disruption in ESX-1 function in Rv-D981 and further suggest a loss of regulatory controls on export of specific ESX-1 substrates.

Altered cytokine induction. ESAT-6 promotes secretion of the proinflammatory interleukin 1β (IL-1β) by macrophages

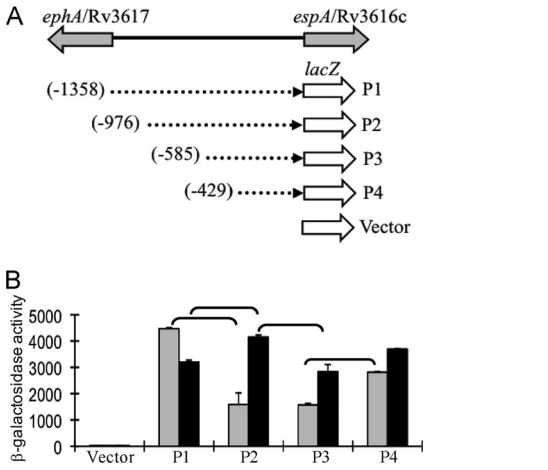

FIG 4 *espA* promoter analysis using *lacZ* reporter constructs. (A) Schematic representation of promoter constructs generated from the *ephA-espA* intergenic region. Dashed lines indicate sections inserted upstream of *lacZ* in constructs P1 to P4. Numbers indicate the starting position relative to the *espA* start codon. P1 contains the full intergenic region. "Vector" represents the promoterless *lacZ* control plasmid pSM128. (B) H37Rv and Rv-D981 were transformed with the *lacZ* promoter constructs, and β-galactosidase activity was measured in Miller units. Gray bars, H37Rv; black bars, Rv-D981. Data are the mean of two experiments ± SD. Statistically significant differences ($P < 0.05$) between constructs in a given strain were determined using an unpaired two-tailed *t* test and are indicated by horizontal brackets.

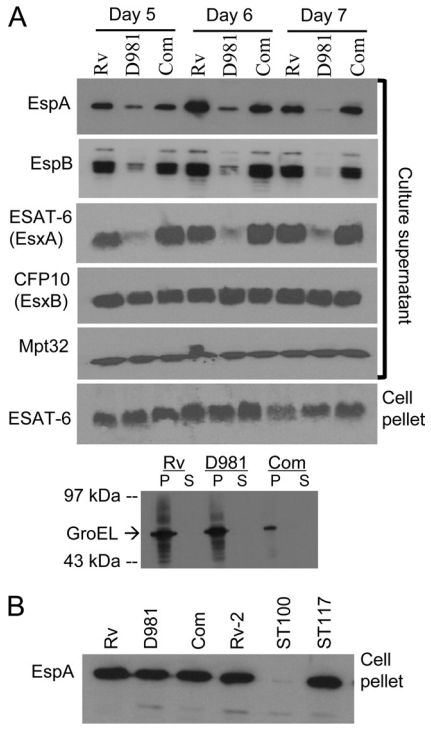

FIG 5 Secretion of ESX-1 substrate proteins is dysregulated in Rv-D981. (A, B) Western blot analyses. Culture supernatants (filtrates) and lysates of cell pellets were analyzed using 5 μg of total protein for each sample. Blots were probed with antibodies to the indicated proteins, followed by a secondary antibody conjugated with horseradish peroxidase. Rv, H37Rv; D981, Rv-D981; Com, Rv-D981COM. (A) Strains were grown in Sauton's medium for 5, 6, or 7 days. Mpt32, a substrate of the Sec pathway that is exported independently of ESX-1, was used as a control for secreted proteins. GroEL was used as the control for lysis of cells during growth, using day 7 cultures. P, pellet; S, supernatant. (B) Comparison of EspA expression in lysates of Rv-D981, the *phoP* mutant ST100, and control strains. Rv-2 and ST117 are the parental strain of ST100 and the *phoPR*-complemented strain, respectively (27).

through activation of the inflammasome (8). Therefore, we hypothesized that reduced secretion of ESAT-6 by Rv-D981 would lessen macrophage stimulation, thereby diminishing IL-1β secretion. We compared the secretion of IL-1β and other cytokines by human monocyte-derived macrophages infected with Rv-D981 and H37Rv, using MOIs of 5:1 and 10:1 (bacteria/macrophage) (Fig. 6). IL-1β levels remained below detection limits in uninfected control cells. However, in cells infected with H37Rv, IL-1β production was induced by 6 h, increased 3- to 5-fold by 12 h, with further elevation by 24 h, at both MOIs (Fig. 6A). Rv-D981 induced significantly lower levels of IL-1β than H37Rv at 6 h and 24 h at each MOI (Fig. 6A), and levels remained below 100 pg/ml at the MOI of 5:1. Although an MOI of 10:1 was more stimulatory for both strains, Rv-D981 induced lower IL-1β levels at that MOI than H37Rv induced at the lower MOI of 5:1. This weaker induction of the proinflammatory cytokine IL-1β is consistent with the reduced secretion of ESAT-6 by Rv-D981 (Fig. 5A).

We also examined the proinflammatory cytokines tumor necrosis factor alpha (TNF-α) and IL-8 and the anti-inflammatory cytokine IL-10 (Fig. 6B to D). H37Rv and Rv-D981 induced equivalent levels of IL-8 (Fig. 6B). However, similar to IL-1β, Rv-D981 induced significantly less TNF-α than H37Rv at all three time points and at both MOIs (Fig. 6C). Both strains induced relatively small amounts of IL-10 compared to IL-1β and TNF-α, with no significant differences between the two strains (Fig. 6D), indicating that the reduced induction of IL-1β and TNF-α by Rv-D981 was not due to suppression by IL-10.

DISCUSSION

Our analyses reveal a major regulatory connection between MprAB and ESX-1. These findings augment the growing evidence that genes associated with the ESX-1 system contribute to the structure and integrity of the cell envelope. The *espA* operon is activated by thioridazine, an agent that damages the cell envelope (42), and an *espA* mutant was more susceptible to the detergent SDS (19). Furthermore, a recent paper reports that EspR regulates numerous genes involved in cell wall function and that it binds within the Rv0986-to-Rv0989c region (24), part of the *in vivo* genomic island containing *mprAB* (43). MprAB activates the response to envelope stresses through sigma factor SigE and the SigE regulon (22, 31). Genes of the MprAB/SigE regulons are induced by agents or environments that impair the integrity of the cell envelope (22, 31, 35, 44–46), and *sigE* mutants are more susceptible to envelope stress, including thioridazine (42, 44, 45). Using real-time PCR and promoter fusion constructs, we determined that *espA* expression was increased in our *mprAB* deletion mutant Rv-D981. Notably, DNA microarray studies by other groups showed that the *espA* operon was also derepressed in an *mprA* insertion mutant (31) and in an *sigE* mutant (44, 47), with derepression in the *sigE* mutant likely resulting from lower expression of *mprAB* (44).

We identified two TSPs within the *espA* promoter, one between MprA boxes 5 and 6, and one between MprA boxes 6 and 7 (see Fig. S1 in the supplemental material). During preparation of the manuscript, two other laboratories also reported TSPs for *espA* (24, 40), and one of these groups (40) further reported that

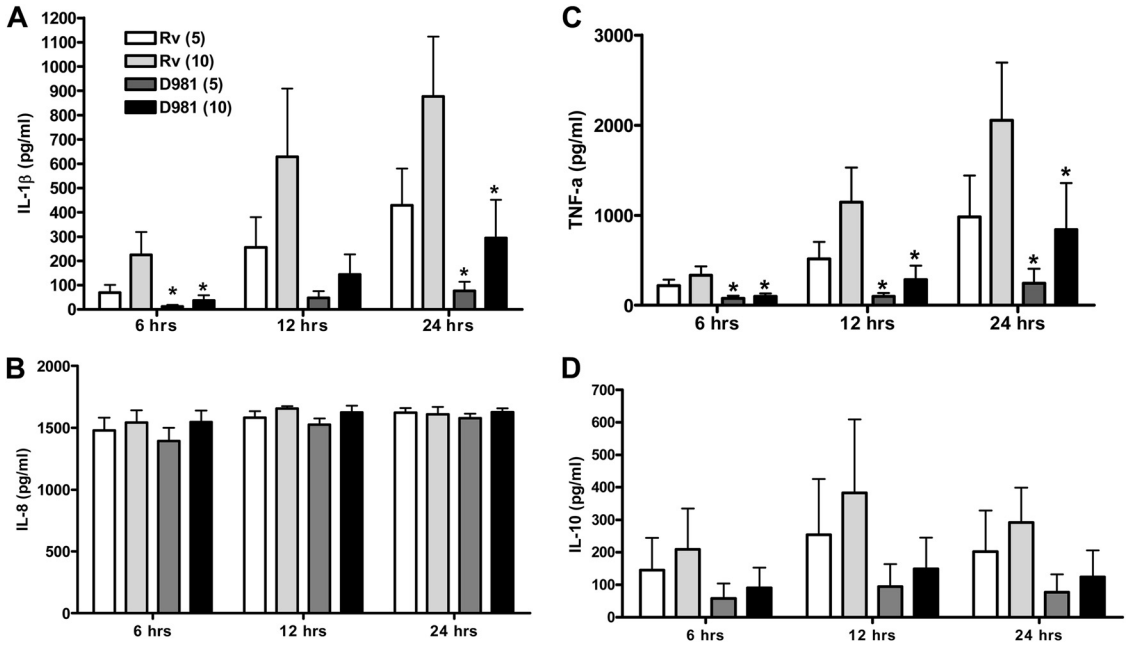

FIG 6 Cytokine production by macrophages infected with Rv-D981 and H37Rv. Monocyte-derived macrophages were isolated from seven healthy donors and infected with H37Rv (Rv) and Rv-D981 (D981) at an MOI of 5:1 or 10:1 (bacteria/monocyte). Culture supernatants were analyzed by ELISA for IL-1β (A), IL-8 (B), TNF-α (C), and IL-10 (D) at 6, 12, and 24 h postinfection. Data are the means ± SD. White bars, H37Rv, MOI of 5:1; light-gray bars, H37Rv, MOI of 10:1; dark-gray bars, Rv-D981, MOI of 5:1; black bars, Rv-D981, MOI of 10:1. Paired Student's *t* test and Wilcoxon matched-pairs signed-rank tests were used for statistical analysis. *, statistically significant difference ($P < 0.05$) between Rv-D981 and H37Rv at the same MOI and time point.

Rv3613c and Rv3612c are part of the *espA* operon, consistent both with our findings and with the coregulation of the five genes in CRP (23) and *mprAB* (22) mutants. Hunt et al. (40) identified the same TSP site for the *espA* operon that we detected at position −67 (TSP1), while Blasco et al. (24) identified a TSP at the adjacent cytosine at position −66. Neither group detected the TSP we found at position −169 (TSP2), but Hunt et al. provided evidence for a potential minor TSP within the *espA* coding region. The basis for the different findings is unclear. However, technical approaches, growth phase of the cultures, and variation among H37Rv strains in different laboratories may be contributing factors. Nevertheless, all three groups identified a major TSP at approximately −67, at least 300 bp away from the nearest EspR activation site (see Fig. S1). EspR generates loops or hairpins within the *espA* promoter (25, 26) that may bring EspR sites closer to the TSPs during activation. More recent analyses (24) indicate that EspR is a nucleoid-associated protein, with the potential for inducing major changes in promoter conformation.

We discovered several potential MprA boxes within the *espA* promoter and confirmed the location of three of these boxes. The derepression of *espA* in Rv-D981 detected by several different experimental approaches suggests that at least some MprA boxes are repressor sites. These sites may function cooperatively to repress *espA*, as suggested by the relatively weak binding of MprA to individual boxes compared to larger promoter probes. Although we hypothesize that MprA directly represses *espA*, further analyses are needed to verify the role of the MprA boxes, as it is possible that MprA represses *espA* indirectly through another repressor protein. Indeed, the unexpectedly low activity from the P1 *lacZ* construct in Rv-D981 suggests that additional factors are at play here. Results with the P4 construct also suggest that other unidentified regulators are involved in modulating *espA* activity. A previous study with reporter constructs reported enhanced transcription from a 427-bp region of the proximal *espA* promoter (40). They proposed that a transcription factor other than EspR activates the region downstream of position −427. Although there are two confirmed MprA boxes in this region, it appears that this factor is neither MprA nor part of the MprA regulon, as activity from the 429-bp (P4) promoter region was higher than that from P3 in both H37Rv and Rv-D981.

EspR site C is the major EspR-activating site (26), and via extensive promoter mapping, Hunt et al. (40) also identified an *espA*-activating region overlapping this site. In confirmation of previous findings (40), we found that deletion of EspR site C produced the greatest drop in promoter activity in H37Rv. This contrasted markedly with Rv-D981, in which the P2 construct generated the highest promoter activity. P2 contains the three strongest MprA boxes (boxes 4, 5, and 6), and these findings are consistent with the hypothesis that MprA directly represses *espA*. Mutational analyses of the individual MprA boxes should help clarify their contributions. However, evidence suggests that MprA box 4 is a key repressor site, as this box was present in construct P2 but not in constructs P3 and P4, which generated smaller expression differences between H37Rv and Rv-D981. Cooperative binding of EspR at site C and other sites is believed to enable transcript initiation at the distant TSPs by bending the *espA* promoter (25, 26, 40). We hypothesize that this bending occludes and thereby inhibits its repression by MprA, so that in the absence of MprA, EspR site C is no longer needed. Given their roles in regulating envelope-associated genes (22, 24, 31), these two regulatory factors may compete or perhaps cooperate at other promoters.

The regulatory effects of MprAB on ESX-1 are likely more

complex than have been determined so far. MprAB may further impact ESX-1 through WhiB6 (Rv3862c), a transcriptional regulator predicted to regulate ESX-1 components (2). *whiB6* was highly upregulated in Rv-D981 under detergent stress (22), and its promoter binds MprA (X. Pang, S. Howard, unpublished data). Analyses by the TB Database (www.tbdb.org) (48) predict that the *espA* promoter contains binding sites for WhiB6 and for Rv0081, a transcription factor regulated by MprA (49). We also identified a potential MprA box in the *esxA* (ESAT-6) promoter (22), and *esxA* was downregulated in a *sigE* mutant (44). These findings connote a strong association between ESX-1 and the MprAB/SigE regulons and are avenues for further study.

MprAB is the second TCS known to regulate ESX-1. There is evidence for at least indirect regulation of ESX-1 by PhoPR. The attenuated strain H37Ra has a point mutation in *phoP* (50), and its weak secretion of ESAT-6 likely results from downregulation of the *espA* operon (27, 50). We detected EspA in lysates of Rv-D981 but not in lysates of the *phoP* mutant ST100, further supporting a role for PhoPR in *espA* regulation and indicating differing regulatory effects of PhoPR and MprAB on ESX-1. Regulation of ESX-1 by two TCSs, by EspR, and by other transcription factors (21, 23, 24, 30) suggests that there is fine-tuning of the system in response to environmental cues. Indeed, Rv3616c to Rv3614c are upregulated by phosphate starvation, a stress response regulated by the SenX3-RegX3 TCS, which also regulates MprAB (51). Direct regulation of the *espA* promoter by RegX3 or PhoP has not been reported. However, our laboratories (33) and He at al. (49) have discovered two promoters directly regulated by MprA and another response regulator, so this potentially occurs with the *espA* promoter as well.

Despite the increased transcription of *espA* in Rv-D981, EspA levels were not elevated, suggesting that there are posttranscriptional controls on EspA production. Additionally, although Rv-D981 secreted lower levels of EspA and ESAT-6, the proteins did not accumulate in lysates of Rv-D981. This finding contrasts with an *espA* mutant which also had impaired secretion but in which ESAT-6 accumulated in cell lysates (17). Either Rv-D981 has aberrant secretion coupled with increased degradation of the proteins in the cell or synthesis of these proteins is reduced in Rv-D981 and the amount of protein maintained within the bacteria is tightly controlled.

ESAT-6 and CFP10 are usually secreted as a heterodimer (10, 11), so we anticipated that CFP10 secretion would also be impaired in the mutant. However, Rv-D981 secreted normal levels of CFP10, indicating pronounced malfunctioning of ESX-1. The structure of the secretory apparatus may be altered in Rv-D981, permitting secretion of unpaired CFP10, which unlike ESAT-6 contains a specialized signal sequence (9). Interestingly, deletion of several ESX-1 genes from *M. marinum* also allowed CFP10 secretion without ESAT-6 (4), suggesting that the aberration in Rv-D981 results from reduced synthesis of other ESX-1 proteins. However, similar to EspD (16), CFP10 may also be secreted by mechanisms independent of ESX-1.

mprA mutants have enhanced growth in macrophages (22, 52). The basis for this hypergrowth phenotype is unknown and is surprising in view of the decreased secretion of ESAT-6, EspA, and EspB, all virulence factors (5, 11, 19, 53). However, Rv-D981 secretes low levels of these proteins, and perhaps this is sufficient for some functions. Additionally, upregulation of other virulence and stress-associated genes (22) may compensate for diminished ESAT-6 secretion, particularly in the context of the weaker cytokine response induced by Rv-D981. In contrast to the growth profile in macrophages, an *mprA* mutant had reduced survival during chronic infection of mice (52). ESX-1 mutants are normally impaired early during infection (5, 11, 17, 21), so it will be interesting to determine whether malfunction of the ESX-1 system is a factor in the decline of the mutant at the later stage.

M. tuberculosis stimulates cytokine production through the interaction of bacterial components with macrophage pattern recognition receptors, including TLR2 and TLR4 (54, 55). This interaction triggers the synthesis of an inactive form of the proinflammatory cytokine IL-1β (56). Proteolytic cleavage and release of mature IL-1β involves activated inflammasomes (56, 57), and secretion of ESAT-6 is necessary for this activation by *M. tuberculosis* (7, 8). Weaker induction of IL-1β by macrophages infected with Rv-D981 is consistent with the reduced secretion of ESAT-6 and indicates a less robust stimulation of the inflammasome by this mutant. Mature IL-1β appears critical for controlling *M. tuberculosis* infection (58), so it seems contradictory that ESAT-6 would both stimulate IL-1β and yet be a major virulence factor. However, activation of the inflammasome can exacerbate mycobacterial disease (59), and the outcome of infection is likely influenced by multiple host and bacterial factors.

In conclusion, we demonstrate that MprAB directly regulates the *espA* operon and that deletion of *mprAB* disrupts ESX-1 function and modulates the macrophage cytokine response. These studies are further evidence that regulation of ESX-1 is complex and multifactorial and provide new insights into the role of MprAB in the pathogenesis of *M. tuberculosis*.

ACKNOWLEDGMENTS

We thank G. Marcela Rodriguez and Issar Smith for the *M. tuberculosis phoP* mutant ST100 and control strains. We are grateful to Peter Barnes, Jeffery Cox, and Cole Dovey for helpful discussion and Yuanxin Gu and Peipei Zhang for technical assistance. Peter Andersen, Sarah Fortune, and BEI Resources kindly provided antibodies.

This work was supported by the Natural Science Foundation of China (NSFC81071328 and NFSC81171540 to X.P.), the Shandong Provincial Natural Science Foundation (ZR2010HM007 to X.P.), the National Institutes of Health (AI082335 to B.S. and AI063229 to S.T.H.), and the Potts Memorial Foundation (to X.P. and S.T.H). S.T.H. is also supported by the Department of Microbiology at UTHSCT.

REFERENCES

1. **Ligon LS, Hayden JD, Braunstein M.** 2012. The ins and outs of *Mycobacterium tuberculosis* protein export. Tuberculosis (Edinb.) **92**:121–123.
2. **Das C, Ghosh TS, Mande SS.** 2011. Computational analysis of the ESX-1 region of *Mycobacterium tuberculosis*: insights into the mechanism of type VII secretion system. PLoS One **6**:e27980. doi:10.1371/journal.pone.0027980.
3. **Samten B, Wang X, Barnes PF.** 2011. Immune regulatory activities of early secreted antigenic target of 6-kD protein of *Mycobacterium tuberculosis* and implications for tuberculosis vaccine design. Tuberculosis (Edinb.) **91**(Suppl 1):S114–S118.
4. **Gao LY, Guo S, McLaughlin B, Morisaki H, Engel JN, Brown EJ.** 2004. A mycobacterial virulence gene cluster extending RD1 is required for cytolysis, bacterial spreading and ESAT-6 secretion. Mol. Microbiol. **53**:1677–1693.
5. **Hsu T, Hingley-Wilson SM, Chen B, Chen M, Dai AZ, Morin PM, Marks CB, Padiyar J, Goulding C, Gingery M, Eisenberg D, Russell RG, Derrick SC, Collins FM, Morris SL, King CH, Jacobs WR, Jr.** 2003. The primary mechanism of attenuation of bacillus Calmette-Guérin is a loss of secreted lytic function required for invasion of lung interstitial tissue. Proc. Natl. Acad. Sci. U. S. A. **100**:12420–12425.

6. **Samten B, Wang X, Barnes PF.** 2009. *Mycobacterium tuberculosis* ESX-1 system-secreted protein ESAT-6 but not CFP10 inhibits human T-cell immune responses. Tuberculosis (Edinb.) **89**(Suppl 1):S74–S76.
7. **Koo IC, Wang C, Raghavan S, Morisaki JH, Cox JS, Brown EJ.** 2008. ESX-1-dependent cytolysis in lysosome secretion and inflammasome activation during mycobacterial infection. Cell. Microbiol. **10**:1866–1878.
8. **Mishra BB, Moura-Alves P, Sonawane A, Hacohen N, Griffiths G, Moita LF, Anes E.** 2010. *Mycobacterium tuberculosis* protein ESAT-6 is a potent activator of the NLRP3/ASC inflammasome. Cell. Microbiol. **12**: 1046–1063.
9. **Champion PA, Stanley SA, Champion MM, Brown EJ, Cox JS.** 2006. C-terminal signal sequence promotes virulence factor secretion in *Mycobacterium tuberculosis.* Science **313**:1632–1636.
10. **Renshaw PS, Panagiotidou P, Whelan A, Gordon SV, Hewinson RG, Williamson RA, Carr MD.** 2002. Conclusive evidence that the major T-cell antigens of the *Mycobacterium tuberculosis* complex ESAT-6 and CFP-10 form a tight, 1:1 complex and characterization of the structural properties of ESAT-6, CFP-10, and the ESAT-6*CFP-10 complex. Implications for pathogenesis and virulence. J. Biol. Chem. **277**:21598–21603.
11. **Stanley SA, Raghavan S, Hwang WW, Cox JS.** 2003. Acute infection and macrophage subversion by *Mycobacterium tuberculosis* require a specialized secretion system. Proc. Natl. Acad. Sci. U. S. A. **100**:13001–13006.
12. **Guinn KM, Hickey MJ, Mathur SK, Zakel KL, Grotzke JE, Lewinsohn DM, Smith S, Sherman DR.** 2004. Individual RD1-region genes are required for export of ESAT-6/CFP-10 and for virulence of *Mycobacterium tuberculosis.* Mol. Microbiol. **51**:359–370.
13. **Pym AS, Brodin P, Majlessi L, Brosch R, Demangel C, Williams A, Griffiths KE, Marchal G, Leclerc C, Cole ST.** 2003. Recombinant BCG exporting ESAT-6 confers enhanced protection against tuberculosis. Nat. Med. **9**:533–539.
14. **Bottai D, Majlessi L, Simeone R, Frigui W, Laurent C, Lenormand P, Chen J, Rosenkrands I, Huerre M, Leclerc C, Cole ST, Brosch R.** 2011. ESAT-6 secretion-independent impact of ESX-1 genes *espF* and *espG1* on virulence of *Mycobacterium tuberculosis.* J. Infect. Dis. **203**:1155–1164.
15. **Lewis KN, Liao R, Guinn KM, Hickey MJ, Smith S, Behr MA, Sherman DR.** 2003. Deletion of RD1 from *Mycobacterium tuberculosis* mimics bacille Calmette-Guérin attenuation. J. Infect. Dis. **187**:117–123.
16. **Chen JM, Boy-Röttger S, Dhar N, Sweeney N, Buxton RS, Pojer F, Rosenkrands I, Cole ST.** 2012. EspD is critical for the virulence-mediating ESX-1 secretion system in *Mycobacterium tuberculosis.* J. Bacteriol. **194**:884–893.
17. **Fortune SM, Jaeger A, Sarracino DA, Chase MR, Sassetti CM, Sherman DR, Bloom BR, Rubin EJ.** 2005. Mutually dependent secretion of proteins required for mycobacterial virulence. Proc. Natl. Acad. Sci. U. S. A. **102**:10676–10681.
18. **MacGurn JA, Raghavan S, Stanley SA, Cox JS.** 2005. A non-RD1 gene cluster is required for Snm secretion in *Mycobacterium tuberculosis.* Mol. Microbiol. **7**:1653–1663.
19. **Garces A, Atmakuri K, Chase MR, Woodworth JS, Krastins B, Rothchild AC, Ramsdell TL, Lopez MF, Behar SM, Sarracino DA, Fortune SM.** 2010. EspA acts as a critical mediator of ESX1-dependent virulence in *Mycobacterium tuberculosis* by affecting bacterial cell wall integrity. PLoS Pathog. **6**:e1000957. doi:10.1371/journal.ppat.1000957.
20. **Champion PA, Champion MM, Manzanillo P, Cox JS.** 2009. ESX-1 secreted virulence factors are recognized by multiple cytosolic AAA ATPases in pathogenic mycobacteria. Mol. Microbiol. **73**:950–962.
21. **Raghavan S, Manzanillo P, Chan K, Dovey C, Cox JS.** 2008. Secreted transcription factor controls *Mycobacterium tuberculosis* virulence. Nature **454**:717–721.
22. **Pang X, Vu P, Byrd TF, Ghanny S, Soteropoulos P, Mukamolova GV, Wu S, Samten B, Howard ST.** 2007. Evidence for complex interactions of stress-associated regulons in an *mprAB* deletion mutant of *Mycobacterium tuberculosis.* Microbiology **153**:1229–1242.
23. **Rickman L, Scott C, Hunt DM, Hutchinson T, Menéndez MC, Whalan R, Hinds J, Colston MJ, Green J, Buxton RS.** 2005. A member of the cAMP receptor protein family of transcription regulators in *Mycobacterium tuberculosis* is required for virulence in mice and controls transcription of the *rpfA* gene coding for a resuscitation promoting factor. Mol. Microbiol. **5**:1274–1286.
24. **Blasco B, Chen JM, Hartkoorn R, Sala C, Uplekar S, Rougemont J, Pojer F, Cole ST.** 2012. Virulence regulator EspR of *Mycobacterium tuberculosis* is a nucleoid-associated protein. PLoS Pathog. **8**:e1002621. doi: 10.1371/journal.ppat.1002621.
25. **Blasco B, Stenta M, Alonso-Sarduy L, Dietler G, Peraro MD, Cole ST, Pojer F.** 2011. Atypical DNA recognition mechanism used by the EspR virulence regulator of *Mycobacterium tuberculosis.* Mol. Microbiol. **82**: 251–264.
26. **Rosenberg OS, Dovey C, Tempesta M, Robbins RA, Finer-Moore JS, Stroud RM, Cox JS.** 2011. EspR, a key regulator of *Mycobacterium tuberculosis* virulence, adopts a unique dimeric structure among helix-turn-helix proteins. Proc. Natl. Acad. Sci. U. S. A. **108**:13450–13455.
27. **Walters SB, Dubnau E, Kolesnikova I, Laval F, Daffe M, Smith I.** 2006. The *Mycobacterium tuberculosis* PhoPR two-component system regulates genes essential for virulence and complex lipid biosynthesis. Mol. Microbiol. **60**:312–330.
28. **Abramovitch RB, Rohde KH, Hsu FF, Russell DG.** 2011. *aprABC*: a *Mycobacterium tuberculosis* complex-specific locus that modulates pH-driven adaptation to the macrophage phagosome. Mol. Microbiol. **80**: 678–694.
29. **Fisher MA, Plikaytis BB, Shinnick TM.** 2002. Microarray analysis of the *Mycobacterium tuberculosis* transcriptional response to the acidic conditions found in phagosomes. J. Bacteriol. **184**:4025–4032.
30. **Gordon BR, Li Y, Wang L, Sintsova A, van Bakel H, Tian S, Navarre WW, Xia B, Liu J.** 2010. Lsr2 is a nucleoid-associated protein that targets AT-rich sequences and virulence genes in *Mycobacterium tuberculosis.* Proc. Natl. Acad. Sci. U. S. A. **107**:5154–5159.
31. **He H, Hovey R, Kane J, Singh V, Zahrt TC.** 2006. MprAB is a stress-responsive two-component system that directly regulates expression of sigma factors SigB and SigE in *Mycobacterium tuberculosis.* J. Bacteriol. **188**:2134–2143.
32. **He H, Zahrt TC.** 2005. Identification and characterization of a regulatory sequence recognized by *Mycobacterium tuberculosis* persistence regulator MprA. J. Bacteriol. **187**:202–212.
33. **Pang X, Cao G, Neuenschwander PF, Haydel SE, Hou G, Howard ST.** 2011. The β-propeller gene Rv1057 of *Mycobacterium tuberculosis* has a complex promoter directly regulated by both the MprAB and TrcRS two-component systems. Tuberculosis (Edinb.) **91**:S142–S149.
34. **Pang X, Howard ST.** 2007. Regulation of the alpha-crystallin gene *acr2* by the MprAB two-component system of *Mycobacterium tuberculosis.* J. Bacteriol. **189**:6213–6221.
35. **White MJ, He H, Penoske RM, Twining SS, Zahrt TC.** 2010. PepD participates in the mycobacterial stress response mediated through MprAB and SigE. J. Bacteriol. **192**:1498–1510.
36. **Dussurget O, Timm J, Gomez M, Gold B, Yu S, Sabol SZ, Holmes RK, Jacobs WR, Jr, Smith I.** 1999. Transcriptional control of the iron-responsive *fxbA* gene by the mycobacterial regulator IdeR. J. Bacteriol. **181**:3402–3408.
37. **Haydel SE, Clark-Curtiss JE.** 2006. The *Mycobacterium tuberculosis* TrcR response regulator represses transcription of the intracellularly expressed Rv1057 gene, encoding a seven-bladed beta-propeller. J. Bacteriol. **188**: 150–159.
38. **Miller JH.** 1972. Experiments in molecular genetics. Cold Spring Harbor Laboratory Press, Cold Spring Harbor, NY.
39. **Zhang M, Gong J, Yang Z, Samten B, Cave MD, Barnes PF.** 1999. Enhanced capacity of a widespread strain of *Mycobacterium tuberculosis* to grow in human macrophages. J. Infect. Dis. **179**:1213–1217.
40. **Hunt DM, Sweeney NP, Mori L, Whalan RH, Comas I, Norman L, Cortes T, Arnvig KB, Davis EO, Stapleton MR, Green J, Buxton RS.** 2012. Long range transcriptional control of an operon necessary for virulence-critical ESX-1 secretion in *Mycobacterium tuberculosis.* J. Bacteriol. **194**:2307–2320.
41. **Ohol YM, Goetz DH, Chan K, Shiloh MU, Craik CS, Cox JS.** 2010. Mycobacterium tuberculosis MycP1 protease plays a dual role in regulation of ESX-1 secretion and virulence. Cell Host Microbe **7**:210–220.
42. **Dutta NK, Mehra S, Kaushal D.** 2010. A *Mycobacterium tuberculosis* sigma factor network responds to cell-envelope damage by the promising anti-mycobacterial thioridazine. PLoS One **5**:e10069. doi:10.1371/journal.pone.0010069.
43. **Talaat AM, Lyons R, Howard ST, Johnston SA.** 2004. The temporal expression profile of *Mycobacterium tuberculosis* infection in mice. Proc. Natl. Acad. Sci. U. S. A. **101**:4602–4607.
44. **Manganelli R, Voskuil MI, Schoolnik GK, Smith I.** 2001. The *Mycobacterium tuberculosis* ECF sigma factor σ^E: role in global gene expression and survival in macrophages. Mol. Microbiol. **41**:423–437.
45. **Provvedi R, Boldrin F, Falciani F, Palù G, Manganelli R.** 2009. Global

transcriptional response to vancomycin in *Mycobacterium tuberculosis*. Microbiology **155**:1093–1102.
46. **Schnappinger D, Ehrt S, Voskuil MI, Liu Y, Mangan JA, Monahan IM, Dolganov G, Efron B, Butcher PD, Nathan C, Schoolnik GK.** 2003. Transcriptional adaptation of *Mycobacterium tuberculosis* within macrophages: insights into the phagosomal environment. J. Exp. Med. **198**:693–704.
47. **Manganelli R, Fattorini L, Tan D, Iona E, Orefici G, Altavilla G, Cusatelli P, Smith I.** 2004. The extra cytoplasmic function sigma factor σ^E is essential for *Mycobacterium tuberculosis* virulence in mice. Infect. Immun. **72**:3038–3041.
48. **Reddy TB, Riley R, Wymore F, Montgomery P, Decaprio D, Engels R, Gellesch M, Hubble J, Jen D, Jin H, Koehrsen M, Larson L, Mao M, Nitzberg M, Sisk P, Stolte C, Weiner B, White J, Zachariah ZK, Sherlock G, Galagan JE, Ball CA, Schoolnik GK.** 2009. TB database: an integrated platform for tuberculosis research. Nucleic Acids Res. **37**: D499–D508.
49. **He H, Bretl DJ, Penoske RM, Anderson DM, Zahrt TC.** 2011. Components of the Rv0081-Rv0088 locus, which encodes a predicted formate hydrogenlyase complex, are coregulated by Rv0081, MprA, and DosR in *Mycobacterium tuberculosis*. J. Bacteriol. **193**:5105–5118.
50. **Frigui W, Bottai D, Majlessi L, Monot M, Josselin E, Brodin P, Garnier T, Gicquel B, Martin C, Leclerc C, Cole ST, Brosch R.** 2008. Control of *M. tuberculosis* ESAT-6 secretion and specific T cell recognition by PhoP. PLoS Pathog. **4**:e33. doi:10.1371/journal.ppat.0040033.
51. **Rifat D, Bishai WR, Karakousis PC.** 2009. Phosphate depletion: a novel trigger for *Mycobacterium tuberculosis* persistence. J. Infect. Dis. **200**: 1126–1135.
52. **Zahrt TC, Deretic V.** 2001. *Mycobacterium tuberculosis* signal transduction system required for persistent infections. Proc. Natl. Acad. Sci. U. S. A. **98**:12706–12711.
53. **McLaughlin B, Chon JS, MacGurn JA, Carlsson F, Cheng TL, Cox JS, Brown EJ.** 2007. A mycobacterium ESX-1-secreted virulence factor with unique requirements for export. PLoS Pathog. **3**:e105. doi:10.1371/journal.ppat.0030105.
54. **Means TK, Wang S, Lien E, Yoshimura A, Golenbock DT, Fenton MJ.** 1999. Human Toll-like receptors mediate cellular activation by *Mycobacterium tuberculosis*. J. Immunol. **163**:3920–3927.
55. **Thoma-Uszynski S, Stenger S, Takeuchi O, Ochoa MT, Engele M, Sieling PA, Barnes PF, Rollinghoff M, Bolcskei PL, Wagner M, Akira S, Norgard MV, Belisle JT, Godowski PJ, Bloom BR, Modlin RL.** 2001. Induction of direct antimicrobial activity through mammalian Toll-like receptors. Science **291**:1544–1547.
56. **Lamkanfi M, Dixit VM.** 2011. Modulation of inflammasome pathways by bacterial and viral pathogens. J. Immunol. **187**:597–602.
57. **Fantuzzi G, Dinarello CA.** 1999. Interleukin-18 and interleukin-1 beta: two cytokine substrates for ICE (caspase-1). J. Clin. Immunol. **19**:1–11.
58. **Mayer-Barber KD, Barber DL, Shenderov K, White SD, Wilson MS, Cheever A, Kugler D, Hieny S, Caspar P, Núñez G, Schlueter D, Flavell RA, Sutterwala FS, Sher A.** 2010. Caspase-1 independent IL-1beta production is critical for host resistance to *Mycobacterium tuberculosis* and does not require TLR signaling *in vivo*. J. Immunol. **184**:3326–3330.
59. **Carlsson F, Kim J, Dumitru C, Barck KH, Carano RA, Sun M, Diehl L, Brown EJ.** 2010. Host-detrimental role of Esx-1-mediated inflammasome activation in mycobacterial infection. PLoS Pathog. **6**:e1000895. doi: 10.1371/journal.ppat.1000895.